Supplementary Material for

Dynamic screening and recovery of single cells using microfluidics with dual microvalves

Chang Chen[a], Dong Xu[b], Siwei Bai[c], Zhihang Yu[b], Yonggang Zhu[b], Xiao Xing[d] and Huaying Chen[a]*

[a] School of Mechanical Engineering and Automation, Harbin Institute of Technology (Shenzhen), Shenzhen 518055, China.

[b] School of Science, Harbin Institute of Technology (Shenzhen), Shenzhen 518055, China.

[c] Department of Electrical and Computer Engineering, Technical University of Munich, Garching 85748, Germany.

[d] International Collaborative Laboratory of 2D Materials for Optoelectronics Science and Technology of Ministry of Education, College of Optoelectronic Engineering, Shenzhen University, Shenzhen 518060, China.

* Corresponding Author: chenhuaying@hit.edu.cn, Tel: +86 755 8615 3249

1. Analysis of existing sorting technology

Table S1 Comparison of some microfluidic techniques for high-throughput separation/sorting of cell popualtion.

Types	Size limit/dynamic controllability	Size control mechanics	Particle type	Cell viability rate	Number of chip layers / external devices (Instrument complexity)
Microfilter membrane[1]	Lower limit/No	Microfilter	CTCs	71-74%	3/No
Inertial focusing[2]	Both lower and upper limits/No	Inertial forces	Rigid particles, deformable emulsions, and platelets	N/A	1/No
Centrifugation[3]	Lower limits/No	Centrifugal forces	CTCs	>98%	1/No
Deterministic lateral displacement (DLD)[4]	Both lower and upper limits/No	Micropillars	Parasites	N/A	1/No
Pinched flow fractionation (PFF)[5]	Both lower and upper limits/No	Gravity, drag and buoyancy forces	White blood cells and CTCs	N/A	1/No
Image-based flow cytometry[6]	Both lower and upper limits/Yes	Dielectrophoresis	Mouse fibroblast cells and human osteosarcoma cells	N/A	1/Yes

2. Membrane manufacture

Membrane manufacture required specific spin coating. Better flexibility was necessary for the membrane compared to the pneumatic layer and liquid layer, because it needed to withstand the applied pressure load and produce deformation in the experiments. The proportion of curing agent was reduced and the ratio of curing agent to prepolymer mix is 1:25. After surface salinization of the dried silicon wafer, PDMS mixture was poured onto it for spin coating. The membrane thickness was controlled by adjusting spin speed. Afterwards, the wafer was placed in the oven at 60°C for 3 hours to curing the film.

Figure S1(A-B) shows sideview photos of two membranes under a microscope. It was obvious that the membrane thickness changed as the spin speed varied. Spin speed was the most important factor in membrane manufacture and was thus investigated. The relationship between spin speed and membrane thickness is depicted in Figure S1C. The fitting curve in the figure provides a guideline for future membrane manufacture when the mixing ratio was 1:25.

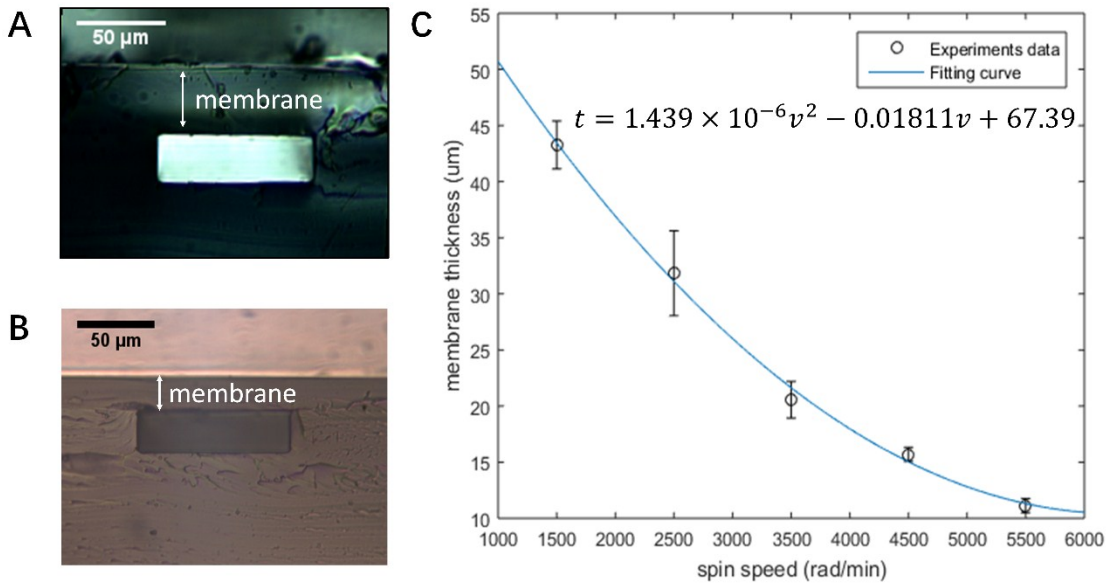

Figure S1 Membrane manufacture and analysis. (A-B) Microscopic views of the microchannel bonding with PDMS membrane spin-coated at (A) 1500 rad/min and (B) 3500rad/min. C. The influence for spin speed to membrane thickness in experiments and its fitting curve.

3. Numerical method

3.1 Boundary condition

The parameters used in this study were summarized in Table S1. The critical model settings were as follows:

a) Boundary load: The values of pressure loaded to the membrane were 1, 2, 3 and 4 atm.

b) Constraint: As shown in Figure S2B, the four outside edges (light blue) of the membrane were set as fixed boundaries, whereas the intersection between the side walls and the membrane were set as elastically supported boundaries. All inside and outside walls of the microchannel were set as elastic supported and fixed boundaries, respectively.

c) The elastic moduli of the membrane and walls were 0.98 MPa and 2.66 MPa, respectively[7].

d) The Poisson's ratio of PDMS was assumed to be 0.47[8].

Table S2 The parameters used in the simulation

Parameters	Symbols	Value/range	Unit
Standard atmospheric pressure	atm	101325	[Pa]
The width of the microchannel	a	25	[μm]
The height of the microchannel	h	25	[μm]
The width of the membrane	W	75	[μm]
The width of the wall	w	25	[μm]
The thickness of the membrane	t	10, 20 and 30	[μm]
Length of membrane	L	25, 50, 100, 150, 200 and 250	[μm]
The elastic modulus of membrane	E_1	0.98	[MPa]
The elastic modulus of walls	E_2	2.66	[MPa]
Poisson's ratio of the model	υ	0.47	1

3.2 Model validation

The numerical study was conducted using COMSOL Multiphysics 5.3. A mesh convergence test was performed to determine the size of mesh elements to acquire accurate results. A model of a fixed square plate was created to study the maximum deformation at various pressure (see Figure S2A). Only less than 3% difference in the maximum deformation was found between our model and one existing study[9]. Subsequent models were created to include a thin plate with two sides elastic supported by PDMS walls and two other sides fixed. A wall thickness study was carried out to validate if the wall thickness had a major influence on the membrane deformation as a result of the pressure from the top membrane. The thickness of the two vertical walls was varied from 25 μm to 2500 μm (see Figure S2C). It was found that even when the wall was 100 times thicker, the maximum displacement did not change significantly (4.3% variation). This confirmed that the model with a 25μm thick PDMS wall was able to well represent the real experiment condition of a microvalve.

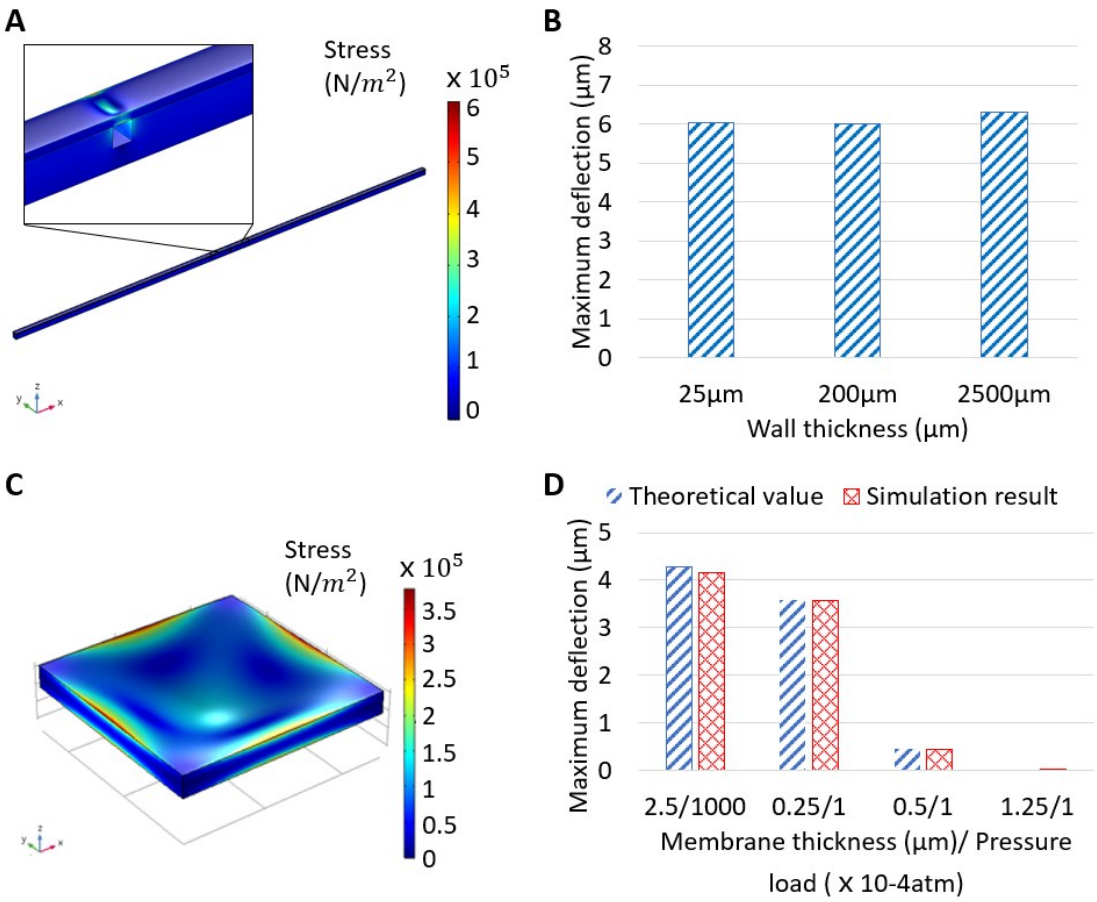

Figure S2 Verification simulations. A. A thicker walls model for wall thickness independence verification. B. Maximum deflection of the membrane with the increase of the wall thickness when the pressure load was 1 atm. C. A simply supported square plate model for method verification. D. Maximum deflection of the membrane when membrane thickness and pressure load varied for fixed model.

4. Analysis study of membrane deformation

The model for coefficient α could be expressed in the form of a quartic polynomial function as below:

$$\alpha = 0.02446 - 0.07758\frac{t}{a} - 0.002961\frac{L}{a} - 0.008296\left(\frac{t}{a}\right)^2 + 0.04701\frac{t \cdot L}{a^2} - 0.002248\left(\frac{t}{a}\right)^2 + 0.0752 - 0.01644\frac{t \cdot L^2}{a^3} + 0.000844\left(\frac{L}{a}\right)^3 - 0.004957\frac{t^2 \cdot L^2}{a^4} + 0.001126\frac{t \cdot L^3}{a^4} - 5.863 \times 10^{-5}\left(\frac{L}{a}\right)^4. \quad (S1)$$

Where α was the coefficient depending on the boundary condition, L/a was the length to width ratio and t/a was the thickness to width ratio.

5. Experimental device

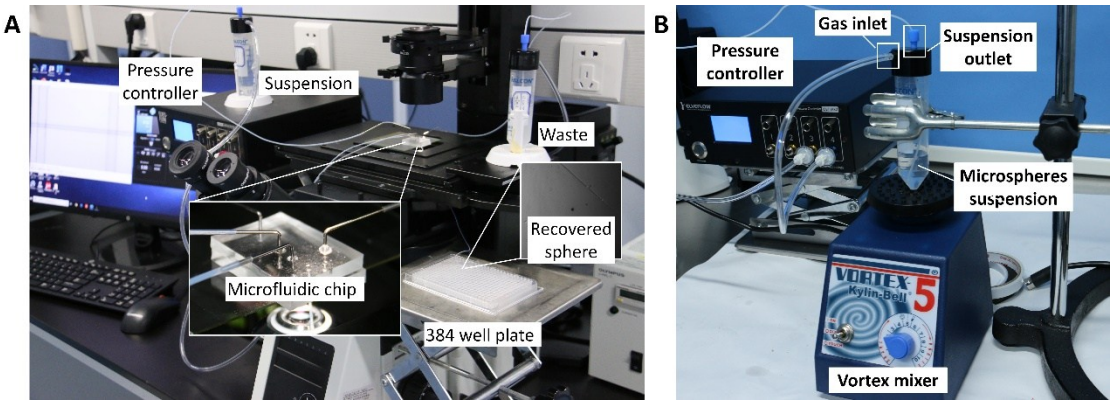

Figure S3 A. Experimental device for dynamic screening and recovery of single cell. B. The device for avoiding aggregation or sedimentation of microspheres in experiments.

6. Cell culture and screening

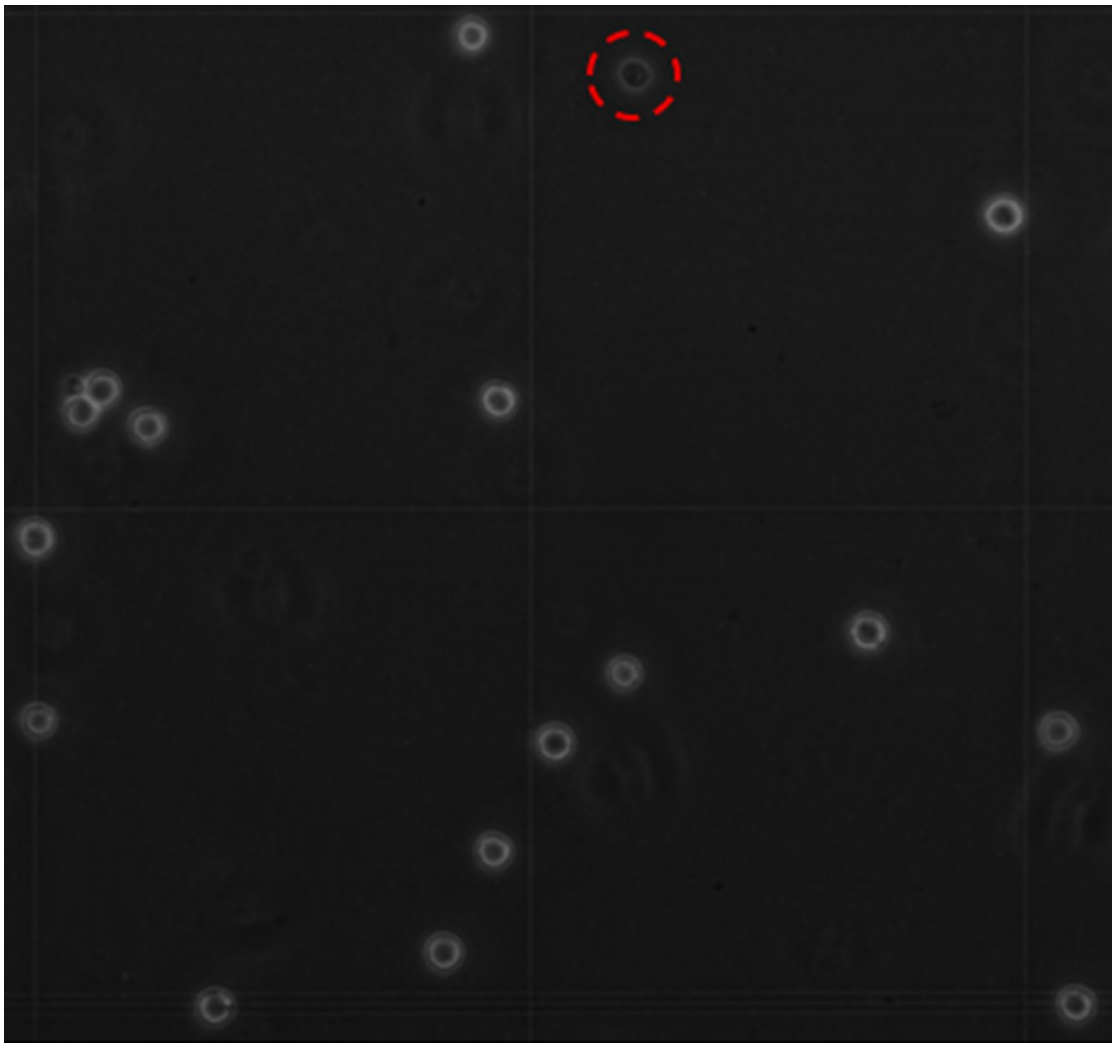

Figure S4 HUVECs in viability experiments, cells that was dashed represent dead cells.

7. Reference

1. M. D. Zhou, S. Hao, A. J. Williams, R. A. Harouaka and S. Y. Zheng, *Sci Rep*, 2014, **5**, 7392.
2. D. D. Carlo, J. F. Edd, D. Irimia, R. G. Tompkins and M. Toner, *Analytical Chemistry*, **80**, 2204-2211.
3. W. H. Han, M. E. Warkiani, B. L. Khoo, R. L. Zi and C. T. Lim, *Sci Rep*, 2013, **3**, 1259.
4. S. H. Holm, J. P. Beech, M. P. Barrett and J. O. Tegenfeldt, *Lab on A Chip*, **11**, 1326.
5. M. Pødenphant, N. Ashley, K. Koprowska, K. U. Mir, M. Zalkovskij, B. Bilenberg, W. Bodmer, A. Kristensen and R. Marie, *Lab on a Chip*, 2015, **15**, 4598-4606.
6. S. H. Ling, Y. C. Lam and K. S. Chian, *Analytical chemistry*, 2012, **84**, 6463-6470.
7. Z. Wang, *Polydimethylsiloxane mechanical properties measured by macroscopic compression and nanoindentation techniques*, University of South Florida, 2011.
8. P. A. Roman, 2004.
9. P. Shen and P. He, *Computers & structures*, 1995, **54**, 1023-1029.